

# Transverse Energy-Energy Correlations in Next-to-Leading Order in $\alpha_s$ at the LHC

Ahmed Ali <sup>a,\*</sup> Fernando Barreiro <sup>b,†</sup> Javier Llorente <sup>b,‡</sup> and Wei Wang <sup>a,§</sup>

*a* Deutsches Elektronen-Synchrotron DESY, D-22607 Hamburg, Germany and

*b* Universidad Autonoma de Madrid (UAM), Facultad de Ciencias C-XI,

Departamento de Física, Cantoblanco, Madrid, Spain

(Dated: October 31, 2021)

We compute the transverse energy-energy correlation (EEC) and its asymmetry (AEEC) in next-to-leading order (NLO) in  $\alpha_s$  in proton-proton collisions at the LHC with the center-of-mass energy  $E_{c.m.} = 7$  TeV. We show that the transverse EEC and the AEEC distributions are insensitive to the QCD factorization- and the renormalization-scales, structure functions of the proton, and for a judicious choice of the jet-size, also the underlying minimum bias events. Hence they can be used to precisely test QCD in hadron colliders and determine the strong coupling  $\alpha_s$ . We illustrate these features by defining the hadron jets using the anti- $k_T$  jet algorithm and an event selection procedure employed in the analysis of jets at the LHC and show the  $\alpha_s(M_Z)$ -dependence of the transverse EEC and the AEEC in the anticipated range  $0.11 \leq \alpha_s(M_Z) \leq 0.13$ .

PACS numbers: 13.87.Ce, 12.38.Bx, 13.85.-t

arXiv:1205.1689v2 [hep-ph] 28 Nov 2012

---

\*ahmed.ali@desy.de

†fernando.barreiro@uam.es

‡javier.llorente.merino@cern.ch

§wei.wang@desy.de

## I. INTRODUCTION

Hadron jets are powerful quantitative tools to study Quantum Chromo Dynamics (QCD) in high energy physics. In  $e^+e^-$  colliders PETRA, PEP and LEP, and also in the electron-proton collider HERA, jet studies have been undertaken extensively. These include the measurements of the inclusive variables, such as thrust, acoplanarity and hadron energy flow, as well as the exclusive jet distributions, yielding a consistent and precise value of the QCD coupling constant  $\alpha_s(M_Z)$  [1]. At the hadron colliders Tevatron and the LHC, QCD predictions for jets have been compared with the measured transverse momentum ( $p_T$ ) distributions, and also with the multi-jet rates [2–4] assuming a jet algorithm [5–7]. The theoretical framework for calculating the jet cross sections in hadronic collisions in the next-to-leading order (NLO) accuracy has been in place for well over a decade [8, 9], which has been employed in the QCD-based analysis of the data.

In comparison to the  $e^+e^-$  and the  $ep$  experiments, event shape variables have so far received less attention in the analysis of the data from the hadron colliders, though first results have been lately published on the measurement of the transverse thrust and the thrust minor distributions [10] by the CDF collaboration [11]. Studies of the hadronic event shapes in  $pp$  collisions at the LHC have just started, initiated by the CMS collaboration using the central transverse thrust and the central transverse minor variables, where the term *central* refers to the jets in the central region of the detector [12]. This is followed by a similar analysis by the ATLAS collaboration [13]. The distributions in these variables have been compared with a number of Monte Carlo (MC) simulations, with PYTHIA6 [14], PYTHIA8 [15] and HERWIG++ [16] providing a good description of the data. However, a bench-mark in this field, namely a quantitative determination of  $\alpha_s(M_Z)$  at the LHC from the analysis of data on event shapes, is still very much a work in progress.

In this paper, we calculate the transverse energy energy correlation and its asymmetry proposed some time ago [17] as a quantitative measure of perturbative QCD in hadronic collisions. The analogous energy-energy correlation (EEC) function measurements - the energy weighted angular distributions of the produced hadron pairs in  $e^+e^-$  annihilation - were proposed by Basham et al. [18]. The EEC and its asymmetry (AEEC) were subsequently calculated in  $O(\alpha_s^2)$  [19, 20], and their measurements have impacted significantly on the precision tests of perturbative QCD and in the determination of  $\alpha_s$  in  $e^+e^-$  annihilation experiments (for a recent review, see [21]). Transverse EEC distributions in hadronic collisions [17], on the other hand, are handicapped due to the absence of the NLO perturbative QCD corrections. In the leading order in  $\alpha_s(\mu)$ , these distributions show marked sensitivities on the renormalization and factorization scales  $\mu = \mu_R$  and  $\mu = \mu_F$ , respectively, thereby hindering a determination of  $\alpha_s(M_Z)$ . We aim at remedying this drawback by presenting a calculation of the transverse EEC function and its asymmetry in  $O(\alpha_s^2(\mu))$ , which reduces the scale-dependence to a few per cent.

The paper is organized as follows. Sec. II collects the definitions and some leading-order features of the transverse energy-energy correlation. In Sec. III, we present the numerical results calculated at next-to-leading order in  $\alpha_s$  and demonstrate that the transverse EEC and its asymmetry are robust against variations of various parameters except for  $\alpha_s$ , for which we present the NLO results in the range  $0.11 < \alpha_s(m_Z) < 0.13$  at the LHC ( $\sqrt{s} = 7\text{TeV}$ ). We conclude in the last section.

## II. TRANSVERSE ENERGY-ENERGY CORRELATION AND ITS ASYMMETRY

We start by recalling the definition of the transverse EEC function [17]

$$\begin{aligned} \frac{1}{\sigma'} \frac{d\Sigma'}{d\phi} &\equiv \frac{\int_{E_T^{\text{min}}}^{\sqrt{s}} dE_T d^2\Sigma/dE_T d\phi}{\int_{E_T^{\text{min}}}^{\sqrt{s}} dE_T d\sigma/dE_T} \\ &= \frac{1}{N} \sum_{A=1}^N \frac{1}{\Delta\phi} \sum_{\text{pairs in } \Delta\phi} \frac{2E_{Ta}^A E_{Tb}^A}{(E_T^A)^2}, \end{aligned} \quad (1)$$

with

$$\sigma' = \int_{E_T^{\text{min}}}^{\sqrt{s}} dE_T d\sigma/dE_T$$

The first sum on the right-hand side in the second of the above equations is over the events A with total transverse energy  $E_T^A = \sum_a E_{T_a}^A \geq E_T^{\min}$ , with the  $E_T^{\min}$  set by the experimental setup. The second sum is over the pairs of partons ( $a, b$ ) whose transverse momenta have relative azimuthal angle  $\phi$  to  $\phi + \Delta\phi$ . In addition, the fiducial volume is restricted by the experimental acceptance in the rapidity variable  $\eta$ .

In leading order QCD, the transverse energy spectrum  $d\sigma/dE_T$  is a convolution of the parton distribution functions (PDFs) with the  $2 \rightarrow 2$  hard scattering partonic sub-processes. Away from the end-points, i.e., for  $\phi \neq 0^\circ$  and  $\phi \neq 180^\circ$ , in the leading order in  $\alpha_s$ , the energy-weighted cross section  $d^2\Sigma/dE_T d\phi$  involves the convolution of the PDFs with the  $2 \rightarrow 3$  sub-processes, such as  $gg \rightarrow ggg$ . Thus, schematically, the leading contribution for the transverse EEC function is calculated from the following expression:

$$\frac{1}{\sigma'} \frac{d\Sigma'}{d\phi} = \frac{\Sigma_{a_i, b_i} f_{a_1/p}(x_1) f_{a_2/p}(x_2) \star \hat{\Sigma}^{a_1 a_2 \rightarrow b_1 b_2 b_3}}{\Sigma_{a_i, b_i} f_{a_1/p}(x_1) f_{a_2/p}(x_2) \star \hat{\sigma}^{a_1 a_2 \rightarrow b_1 b_2}} , \quad (2)$$

where  $\hat{\Sigma}^{a_1 a_2 \rightarrow b_1 b_2 b_3}$  is the transverse energy-energy weighted partonic cross section,  $x_i$  ( $i = 1, 2$ ) are the fractional longitudinal momenta carried by the partons,  $f_{a_1/p}(x_1)$  and  $f_{a_2/p}(x_2)$  are the PDFs, and the  $\star$  denotes a convolution over the appropriate variables. The function defined in Eq. (2) depends not only on  $\phi$ , but also on the ratio  $E_T^{\min}/\sqrt{s}$  and rapidity  $\eta$ . In general, the numerator and the denominator in Eq. (2) have a different dependence on these variables, as the PDFs are weighted differently. However, as already observed in [17], certain *normalized* distributions for the various sub-processes contributing to the  $2 \rightarrow 3$  hard scatterings are similar, and the *same* combination of PDFs enters in the  $2 \rightarrow 2$  and  $2 \rightarrow 3$  cross sections; hence the transverse EEC cross section is to a good approximation *independent* of the PDFs (see, Fig. 1 in [17]). Thus, for a fixed rapidity range  $|\eta| < \eta_c$  and the variable  $E_T/\sqrt{s}$ , one has an approximate factorized result, which in the LO in  $\alpha_s$  reads as

$$\frac{1}{\sigma'} \frac{d\Sigma'}{d\phi} \sim \frac{\alpha_s(\mu)}{\pi} F(\phi) , \quad (3)$$

where

$$\alpha_s(\mu) = \frac{1}{b_0 \log(\mu^2/\Lambda^2)} \left[ 1 - \frac{b_1 \log(\log(\mu^2/\Lambda^2))}{b_0^2 \log(\mu^2/\Lambda^2)} \right], \quad b_0 = \frac{33 - 12n_f}{12\pi}, \quad b_1 = \frac{153 - 19n_f}{24\pi^2}. \quad (4)$$

In the above equation,  $n_f$  is the active quark flavor number at the scale  $\mu$  and the hadronization scale  $\Lambda$  is determined by the input  $\alpha_s(m_Z)$ . The function  $F(\phi)$  and the corresponding transverse EEC asymmetry defined as

$$\frac{1}{\sigma'} \frac{d\Sigma'^{\text{asym}}}{d\phi} \equiv \frac{1}{\sigma'} \frac{d\Sigma'}{d\phi} \Big|_{\phi} - \frac{1}{\sigma'} \frac{d\Sigma'}{d\phi} \Big|_{\pi-\phi} , \quad (5)$$

were worked out in [17] in the leading order of  $\alpha_s$  for the CERN SPS  $p\bar{p}$  collider at  $\sqrt{s} = 540$  GeV. In particular, it was shown that the transverse EEC functions for the  $gg$ -,  $gq$ - and  $q\bar{q}$ -scatterings had very similar shapes, and their relative contributions were found consistent to a good approximation with the ratio of the corresponding color factors 1:4/9:16/81 for the  $gg$ ,  $gq(=g\bar{q})$  and  $q\bar{q}$  initial states over a large range of  $\phi$ .

### III. NEXT-TO-LEADING ORDER RESULTS FOR THE TRANSVERSE EEC AND ITS ASYMMETRY

We have used the existing program NLOJET++ [9], which has been checked in a number of independent NLO jet calculations [22], to compute the transverse EEC and its asymmetry AEEC in the NLO accuracy for the LHC proton-proton center-of-mass energy  $\sqrt{s} = 7$  TeV. Schematically, this entails the calculations of the  $2 \rightarrow 3$  partonic sub-processes in the NLO accuracy and of the  $2 \rightarrow 4$  partonic processes in the leading order in  $\alpha_s(\mu)$ , which contribute to the numerator on the r.h.s. of Eq. (2). We have restricted the azimuthal angle range by cutting out regions near  $\phi = 0^\circ$  and  $\phi = 180^\circ$ . This would, in particular, remove the self-correlations ( $a = b$ ) and frees us from calculating the  $O(\alpha_s^2)$  (or two-loop) virtual corrections to the  $2 \rightarrow 2$  processes. Thus, with the azimuthal angle cut, the numerator in Eq. (2) is calculated from the  $2 \rightarrow 3$  and  $2 \rightarrow 4$  processes to  $O(\alpha_s^4)$ . The denominator in Eq. (2) includes the  $2 \rightarrow 2$  and  $2 \rightarrow 3$  processes, which are calculated up to and including the  $O(\alpha_s^3)$  corrections.

In the NLO accuracy, one can express the EEC cross section as

$$\frac{1}{\sigma'} \frac{d\Sigma'}{d\phi} \sim \frac{\alpha_s(\mu)}{\pi} F(\phi) \left[ 1 + \frac{\alpha_s(\mu)}{\pi} G(\phi) \right] . \quad (6)$$

It is customary to lump the NLO corrections in a so-called  $K$ -factor (which, as shown here, is a non-trivial function of  $\phi$ ), defined as

$$K^{\text{EEC}}(\phi) \equiv 1 + \frac{\alpha_s(\mu)}{\pi} G(\phi) . \quad (7)$$

The transverse EEC asymmetry in the NLO accuracy is likewise defined as

$$\frac{1}{\sigma'} \frac{d\Sigma'^{\text{asym}}}{d\phi} \sim \frac{\alpha_s(\mu)}{\pi} A(\phi) \left[ 1 + \frac{\alpha_s(\mu)}{\pi} B(\phi) \right] . \quad (8)$$

and the corresponding K-factor is defined as

$$K^{\text{AEEC}}(\phi) \equiv 1 + \frac{\alpha_s(\mu)}{\pi} B(\phi) . \quad (9)$$

The principal result of this paper is the calculation of the NLO functions  $K^{\text{EEC}}(\phi)$  and  $K^{\text{AEEC}}(\phi)$  and in demonstrating the insensitivity of the EEC and the AEEC functions, calculated to NLO accuracy, to the various intrinsic parametric and the underlying event uncertainties.

We now give details of the computations: In transcribing the NLOJET++ [9] program, we have replaced the default structure functions therein by the state of the art PDFs, for which we use the MSTW [23] and the CT10 [24] sets. We have also replaced the  $k_T$  jet algorithm by the anti- $k_T$  jet algorithm [7] for defining the jets, in which the distance measures of partons are given by

$$d_{ij} = \min(k_{ti}^{-2}, k_{tj}^{-2}) \frac{(\eta_i - \eta_j)^2 + (\phi_i - \phi_j)^2}{R^2}, \quad d_{iB} = k_{ti}^{-2}, \quad (10)$$

with  $R$  being the usual radius parameter. We recall that the NLO corrections we are using [9] have been computed in the Catani-Seymour dipole formalism [6]. In particular, it involves a certain cutting of the phase space of the dipole subtraction terms and the numerical calculations require the generation of a very large number of events (we have generated  $O(10^{10})$  events on the DESY-Theory PC Cluster) to bring the statistical accuracy in the NLO EEC distribution to the desired level of below a few per cent. We have assumed the rapidity range  $|\eta| \leq 2.5$ , have put a cut on the transverse energy  $E_T > 25$  GeV for each jet and require  $E_{T1} + E_{T2} > 500$  GeV for the two leading jets. The latter cut ensures that the trigger efficiencies for the LHC detectors will be close to 100%. We have set the transverse energy of the hardest jet as the default factorization- and renormalization-scale, i.e.,  $\mu_F = \mu_R = E_T^{\text{max}}$ . We then vary the scales  $\mu_F$  and  $\mu_R$  independently in the range  $0.5 E_T^{\text{max}} \leq (\mu_F, \mu_R) \leq 2 E_T^{\text{max}}$  to study numerically the scale dependence.

The effects induced by the underlying event, multiparton interactions and hadronization effects have been studied by us using the PYTHIA6 MC [15]. In Fig .1, we show a comparison of the transverse EEC and its asymmetry for  $R=0.6$  and  $R=0.4$  with and without the underlying event effects (UE). In Fig .2, the results of the transverse EEC and its asymmetry at the hadron and parton level are presente for  $R=0.6$  and  $R=0.4$ . To better display this, we show in Fig. 3 the normalized distribution of the hadronization factor (left) and the underlying events factor (right), from which it is easy to see that both the hadronization and the UE effects are small. Typically, the effect of hadronization on the transverse EEC is  $\leq 5\%$  and from the underlying event  $\leq 6\%$  for the jet-size parameter  $R = 0.6$ . The corresponding numbers are  $\leq 5\%$  and  $\leq 2\%$  for  $R = 0.4$ . The parameter specifying the jet-size in the anti- $k_T$  algorithm is chosen as  $R = 0.4$  in the rest of this paper, as this choice makes the transverse EEC distribution less sensitive to the underlying minimum-bias events. Moreover, a smaller value of  $R$  induces smaller distortions on the EEC distribution for the smaller values of the angle  $\phi$ .

An important issue is the effect of the parton showers in the transverse EEC and the AEEC distributions. They are crucially important in the  $\phi \rightarrow 0^\circ$  and  $\phi \rightarrow 180^\circ$  angular regions, but their effect is expected to be small in the central angular range on which we have concentrated. We have checked this (approximately) by comparing the results in the LO accuracy with those from the parton shower-based MC generator PYTHIA6 [15], which is accurate in the leading log approximation and also includes some NLO terms. Matching the NLO computations with the parton shower simulations in the complete next-to-leading log (NLL) accuracy is the aim of several approaches, such as the POWHEG method, pioneered and subsequently developed in [25, 26], which would allow to quantitatively compute the end-point region in the transverse EEC cross section [27]. Likewise, resummed perturbative techniques have been developed in a number of dedicated studies for some event shape variables in hadronic collisions [10, 28], which would expand the domain of applicability of the perturbative techniques to a wider angular region in  $\phi$ .

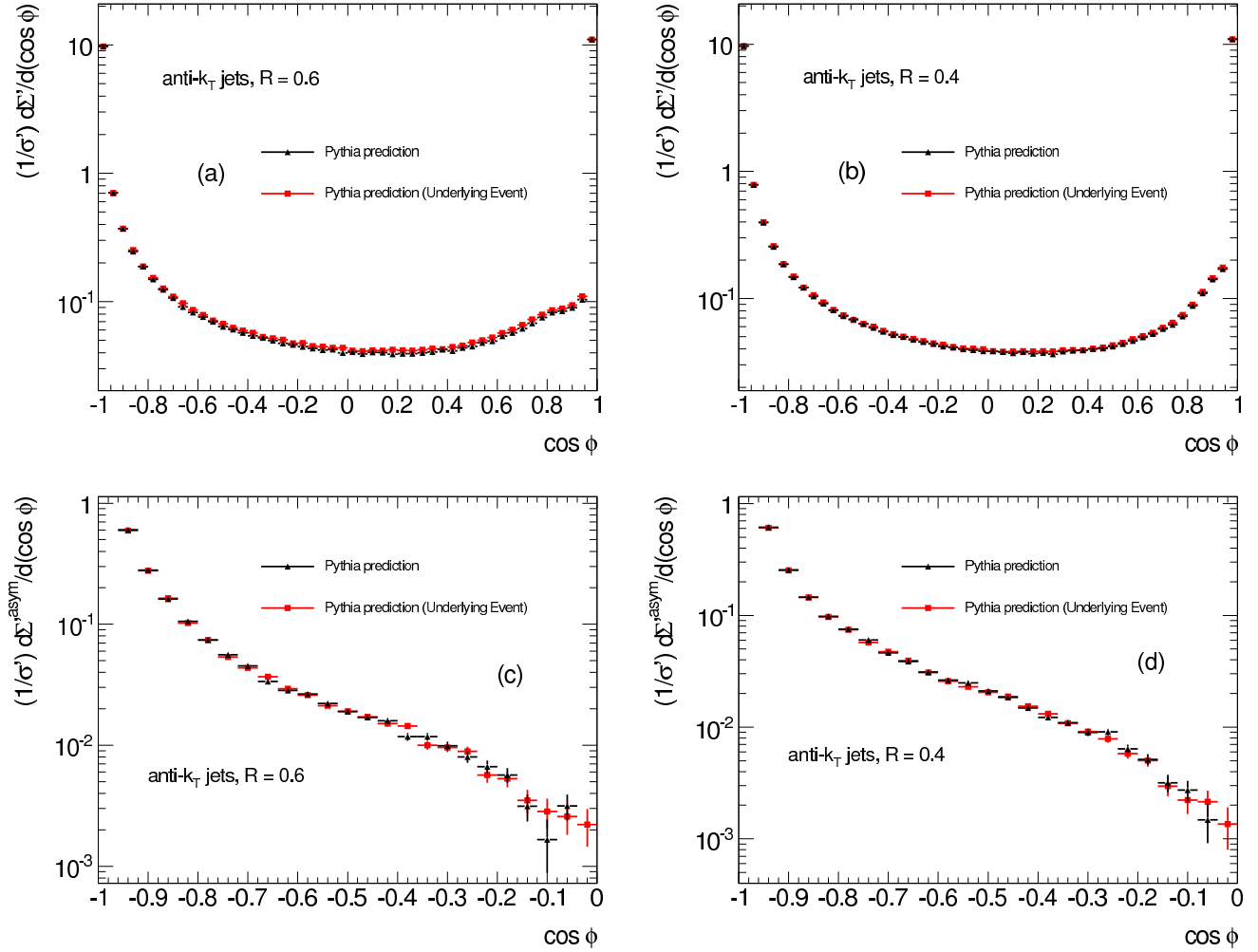


FIG. 1. (color online) Differential distribution in  $\cos \phi$  of the transverse EEC cross section [(a),(b)] and its asymmetry [(c),(d)] obtained with the PYTHIA6 MC program [15] with and without the underlying events at  $\sqrt{s} = 7$  TeV and the anti- $k_T$  algorithm with two assumed values of the jet-size parameter  $R = 0.6$  [(a),(c)] and  $R = 0.4$  [(b),(d)].

In view of the preceding discussion, we have restricted  $\cos \phi$  in the range  $[-0.8, 0.8]$  which is sliced into 20 bins for the presentation of our numerical results. We first show the dependence of the transverse EEC calculated in the NLO accuracy on the PDFs in Fig. 4 for the two widely used sets: MSTW [23] and CT10 [24], using their respective central (default) parameters. This figure shows that the PDF-related differences on the transverse EEC are negligible, with the largest difference found in some bins amounting to 3%, (but typically they are  $< 1\%$ ). We also remark that the intrinsic uncertainties from the MSTW2008 PDFs, taking the first 10 eigenvectors of the PDF sets to evaluate the distributions, are found negligibly small in the transverse EEC (at most a few per mill), while in the case of CT10, these uncertainties are somewhat larger but still below 1% in the EEC. The insensitivity of the transverse EEC cross section to the PDFs provides a direct test of the underlying partonic hard processes. In what follows, we will adopt the MSTW [23] PDF set as it provides a correlated range of  $\alpha_s(M_Z)$  and the structure functions for the current range of interest for  $\alpha_s(M_Z)$ :  $0.11 < \alpha_s(M_Z) < 0.13$ .

We next explore the dependences of the transverse EEC cross section and its asymmetry on the factorization and the renormalization scales in the range  $(\mu_F, \mu_R) = [0.5, 2] \times E_T^{\max}$  and display them in Fig. 5 for the transverse EEC and Fig. 6 for the asymmetric transverse EEC. Effects of the variations in the scales  $\mu_F$  and  $\mu_R$  on the transverse EEC cross section in the LO are shown in Figs. 5 (a), 5(c) and 5 (e), which are obtained by setting the scales  $\mu_F = \mu_R$ , fixing  $\mu_F = E_T^{\max}$  and varying  $\mu_R$ , and fixing  $\mu_R = E_T^{\max}$  and varying  $\mu_F$ , respectively. The corresponding asymmetry

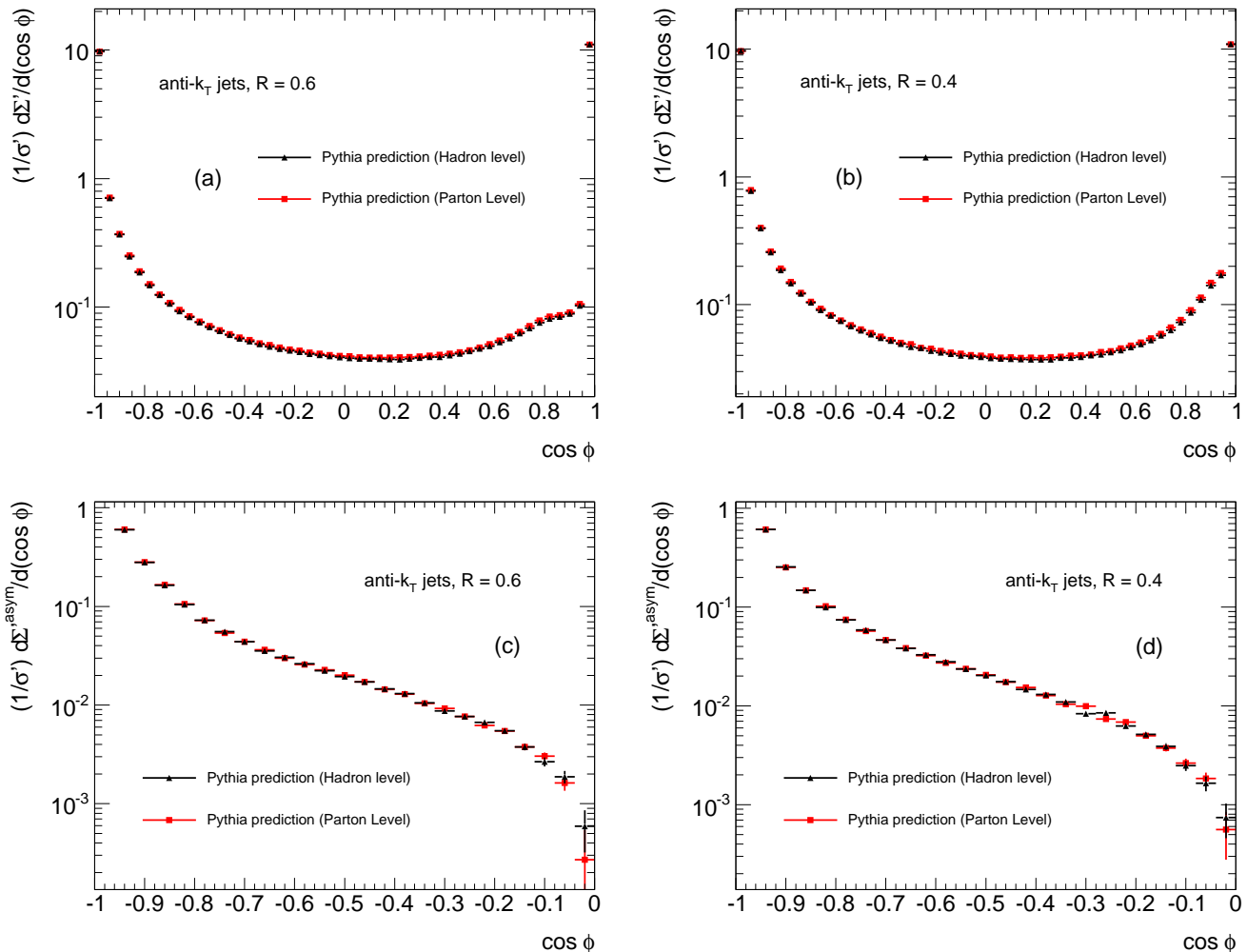


FIG. 2. (color online) Differential distribution in  $\cos \phi$  of the transverse EEC cross section [(a),(b)] and its asymmetry [(c),(d)] obtained with the PYTHIA6 MC program [15] at the hadron and parton level at  $\sqrt{s} = 7$  TeV for the indicated values of the jet-size parameter  $R$ .

of the transverse EEC cross sections are displayed in Figs. 6 (a), 6 (c) and 6 (e). We note that the dominant scale dependence in the LO arises from the variation of the renormalization scale  $\mu_R$ . This is understandable as the LO matrix element have no  $\mu_R$ -compensating contribution. The results obtained in the NLO are shown in Figs. 5 (b), 5 (d) and 5 (f) for the transverse EEC and in Figs. 6 (b), 6 (d) and 6 (f) for the asymmetry. One observes significantly less dependence on the scales; in particular the marked  $\mu_R$ -dependence in the LO is now reduced. Typical scale-variance on the transverse EEC distribution in the NLO is found to be 2% - 3%, with the largest effects in some bins reaching 5%. This scale-insensitivity in the NLO accuracy is crucial to undertake a quantitative determination of  $\alpha_s$  from the collider jet data.

Having shown that the uncertainties due to underlying events and the PDFs are negligible, and the scale dependence is much reduced in the NLO, we present our results for the transverse EEC in the LO and the NLO accuracy in Fig. 7(a), and the corresponding results for the transverse AEEC in Fig. 7 (b). We also compute these distributions from a MC-based model which has the LO matrix elements and multiparton showers encoded. To be specific, we have used the PYTHIA8 [15] MC program and have generated the transverse EEC and the AEEC distributions, which are also shown in Fig. 7(a) and Fig. 7(b), respectively. This comparison provides a practically convenient way to correct the PYTHIA8 MC-based theoretical distributions, often used in the analysis of the hadron collider data, due to the NLO effects. In Fig. 7 (c), we show the function  $K^{\text{EEC}}(\phi)$  defined in Eq. (7) (denoted as NLO/LO in the

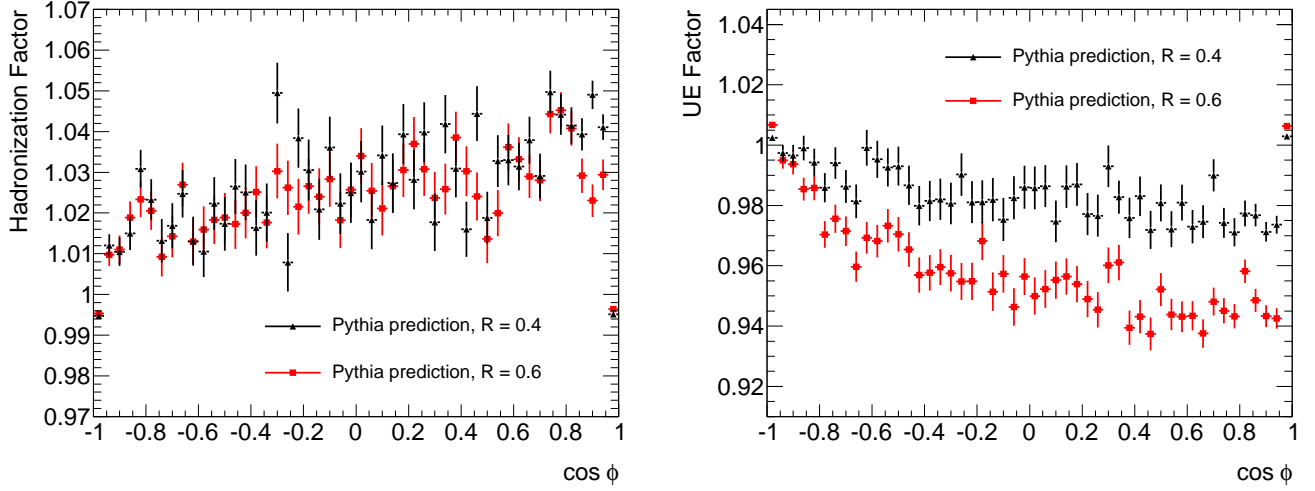


FIG. 3. (color online) Normalized distribution of the hadronization factor (left) and underlying events effects (right) obtained with the PYTHIA6 MC program [15] for the two indicated values of  $R$ .

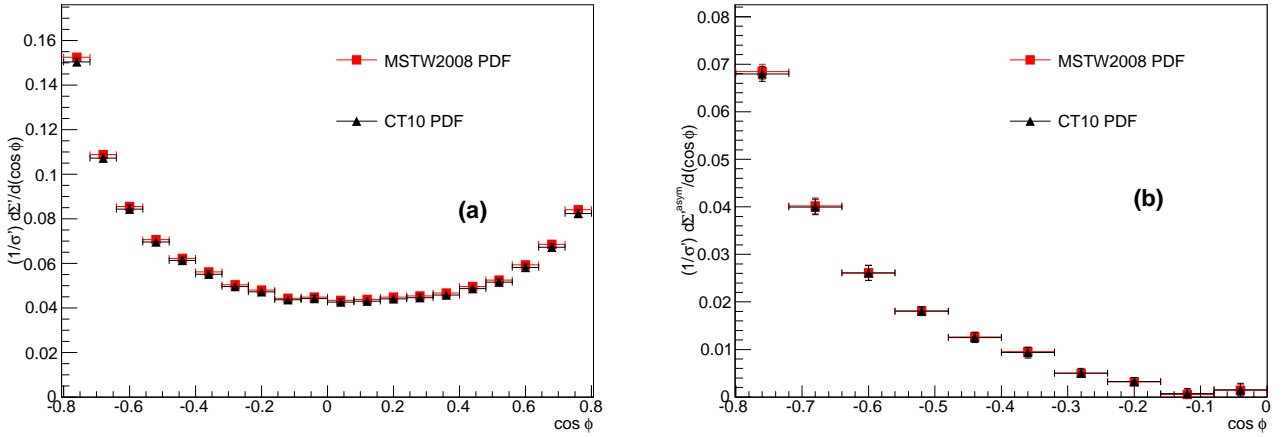


FIG. 4. (color online) Dependence of the transverse EEC cross section (a) and its asymmetry (b) on the PDFs at NLO in  $\alpha_s$ . Red entries correspond to the MSTW [23] PDFs and the black ones are calculated using the CT10 PDF set [24]. The errors shown reflect the intrinsic parametric uncertainties in each PDF set and the Monte Carlo integration uncertainties.

figure) and another phenomenological function in which the NLO transverse EEC distribution is normalized to the one generated by the PYTHIA8 [15] MC program (denoted as NLO/PYTHIA). The corresponding function  $K^{\text{AEEC}}(\phi)$ , defined in Eq. (9), is shown in Fig. 7 (d). Here also we show the corresponding phenomenological function in which the transverse EEC obtained in NLO is normalized to the ones generated by the PYTHIA MC. We remark that the effects of the NLO corrections are discernible, both compared to the LO and PYTHIA8 [15], and they are significant in the large-angle region (i.e., for  $\cos \phi < 0$ ). To summarize the NLO effects in the EEC distribution, they reduce the scale-dependence, in particular on  $\mu_R$ , and distort the shape of both the EEC and AEEC distributions, providing a non-trivial test of the NLO effects.

Having detailed the intrinsic uncertainties from a number of dominant sources, we now wish to investigate the sensitivity of the transverse EEC and the AEEC on  $\alpha_s(M_Z)$ . In relating the strong coupling  $\alpha_s(\mu)$  at a certain scale relevant for the collider jets, such as  $\mu = E_T^{\text{max}}$ , to the benchmark value  $\alpha_s(M_Z)$ , we have used the two-loop  $\beta$ -function and the explicit formula for transcribing  $\alpha_s(\mu)$  to  $\alpha_s(M_Z)$  can be seen in Eq. (4). Results for the transverse

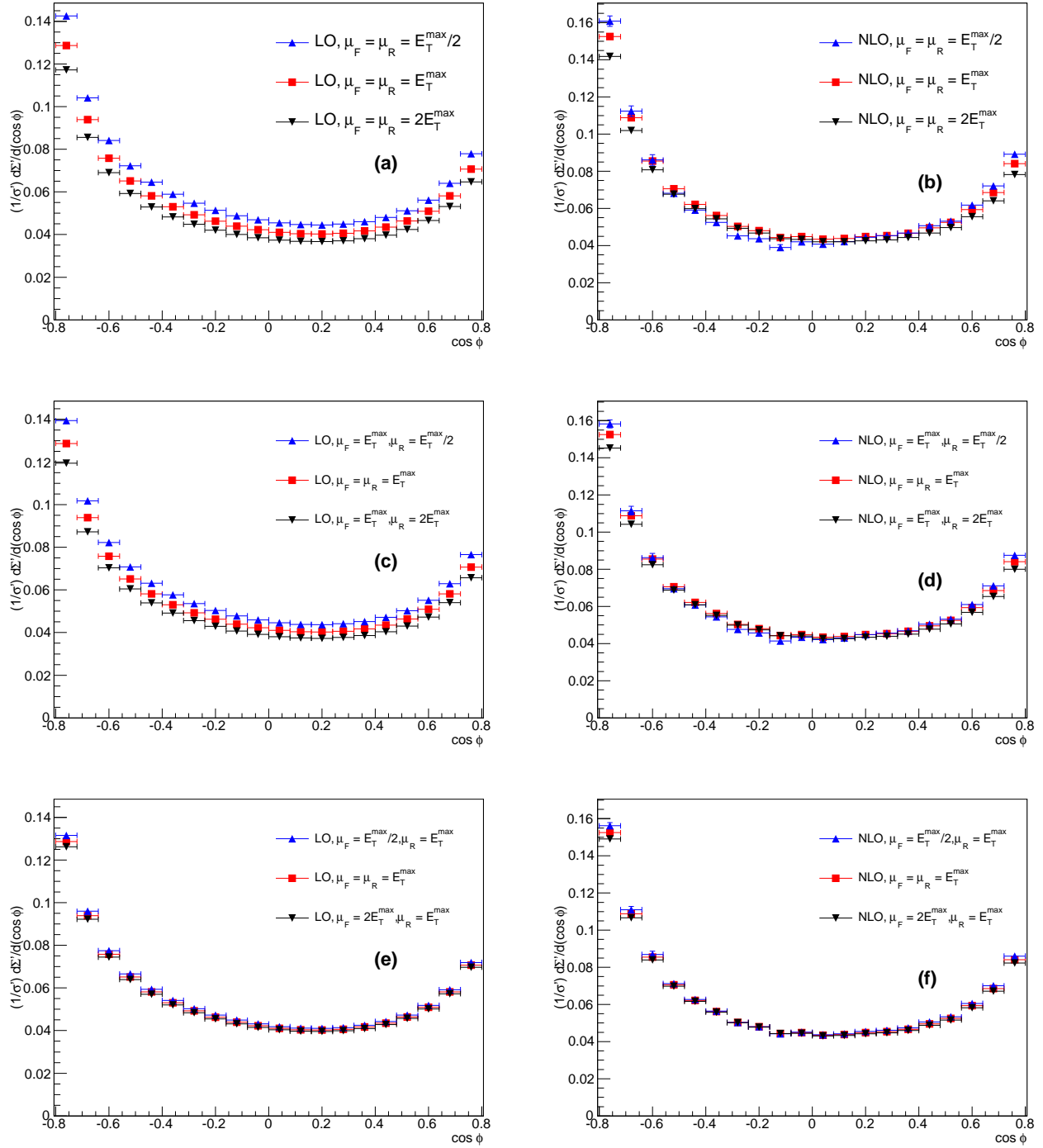


FIG. 5. (color online) Dependence of the transverse EEC on the scales  $\mu_F$ , and  $\mu_R$  in LO (a,c,e) and in the NLO (b,d,f) in  $\alpha_s$  for the indicated values of the scales. Figs.(a) and (b) are obtained by setting  $\mu_F = \mu_R$  and varying it  $\mu_F = \mu_R = [0.5, 2] \times E_T^{\max}$ ; (c) and (d) are obtained by fixing  $\mu_F = E_T^{\max}$  and varying  $\mu_R$ , whereas (e) and (f) are derived varying  $\mu_F$  with fixed  $\mu_R = E_T^{\max}$ .



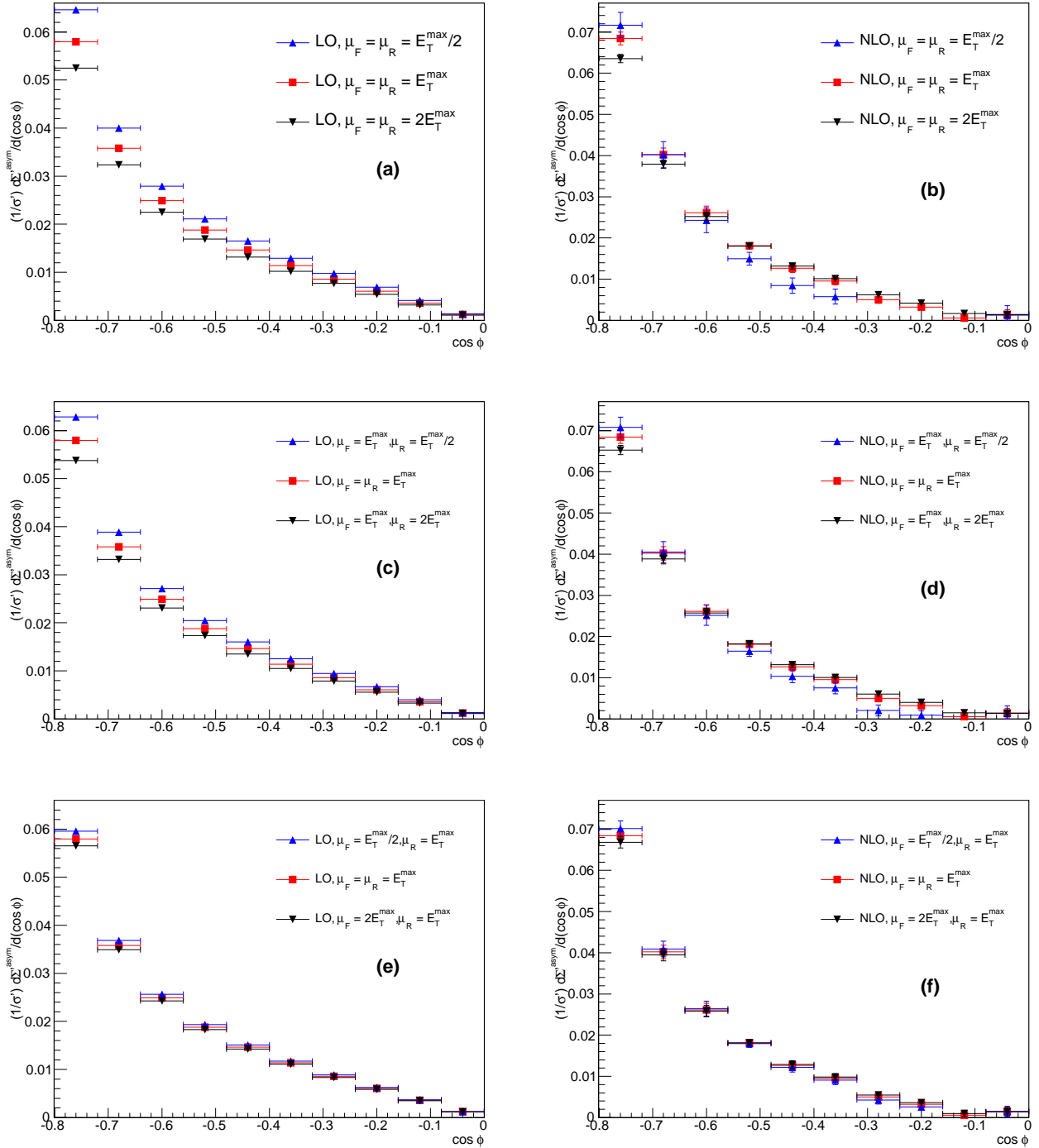


FIG. 6. (color online) Same as Fig. 5 but for the asymmetric transverse EEC.

EEC and the AEEC are shown in Fig. 8 (a) and Fig. 8 (b), respectively, for the three indicated values of  $\alpha_s(M_Z)$ :  $= 0.11$  (blue),  $= 0.12$  (red),  $= 0.13$  (black). The scale uncertainties are included only in the curve corresponding to  $\alpha_s(M_Z) = 0.12$ , as it is close to the current world average  $\alpha_s(M_Z) = 0.1184$  [29] and hence our focus on this value. To demonstrate the intrinsic errors in the calculations of the transverse EEC and its asymmetry, we show the percentage size of the errors in the lower part of Fig. 8 (a) and Fig. 8 (b), respectively, for  $\alpha_s(M_Z) = 0.12$ . Concentrating

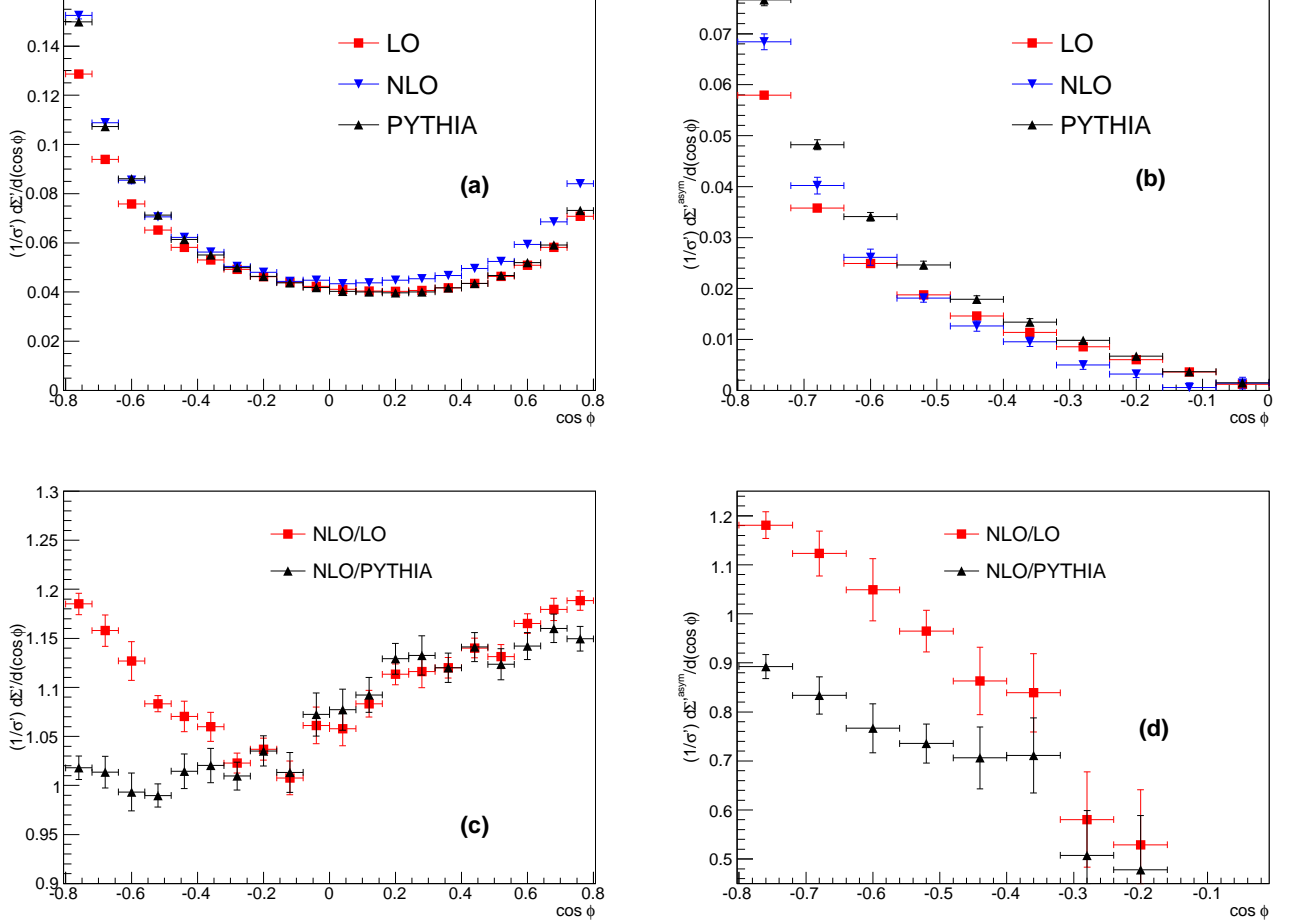


FIG. 7. (color online) Comparison of the LO computation (red entries), NLO calculation (blue entries) and the PYTHIA (black entries) results for the transverse EEC (a) and its asymmetry (b). Fig. (c) displays the function  $K^{\text{EEC}}(\phi)$  involving the ratios NLO/LO (red entries) as defined in Eq. (7) and a phenomenological function obtained by replacing the LO results by the PYTHIA MC results (black entries). Fig. (d) shows the corresponding function  $K^{\text{AEEC}}(\phi)$  for the transverse EEC asymmetry defined in Eq. (9). The errors shown are obtained by adding in quadrature all the uncertainties except the ones from scale variations, as described in text.

first on the transverse EEC, we see that the bin-by-bin errors are typically +2% and -6% (for  $|\cos \phi| \leq 0.6$ ), and somewhat larger for  $|\cos \phi| > 0.6$ . A part of this error is of statistical origin in our Monte Carlo based theoretical calculations and is reducible, in principle, with the help of a more effective importance sampling algorithm in the event generation. However, a part of the error is irreducible, given the current theoretical (NLO) precision. This is quantified for the normalized integrated transverse EEC X-section over the  $\cos \phi$  range shown in the figures above, which largely removes the statistical (bin-by-bin) error:

$$\frac{\alpha_s(m_Z)}{\langle \frac{1}{\sigma'} \frac{d\Sigma'}{d\phi} \rangle} \left| \begin{array}{c|c|c} 0.11 & 0.12 & 0.13 \\ \hline 0.092^{+0.001}_{-0.005} & 0.101^{+0.001}_{-0.005} & 0.111^{+0.001}_{-0.005} \end{array} \right.$$

The computational error on the transverse AEEC is larger, as shown in Fig. 8 (b) for  $\alpha_s(M_Z) = 0.12$ . In particular, the errors for the last four bins in the AEEC X-section are large due to the intrinsically small value of this cross-section as  $\cos \phi \rightarrow 0$ . However, in the region  $-0.8 \leq \cos \phi \leq -0.4$ , a clear dependence of the differential transverse AEEC on  $\alpha_s(M_Z)$  is discernible. This is also displayed for the normalized integrated transverse AEEC X-section given below

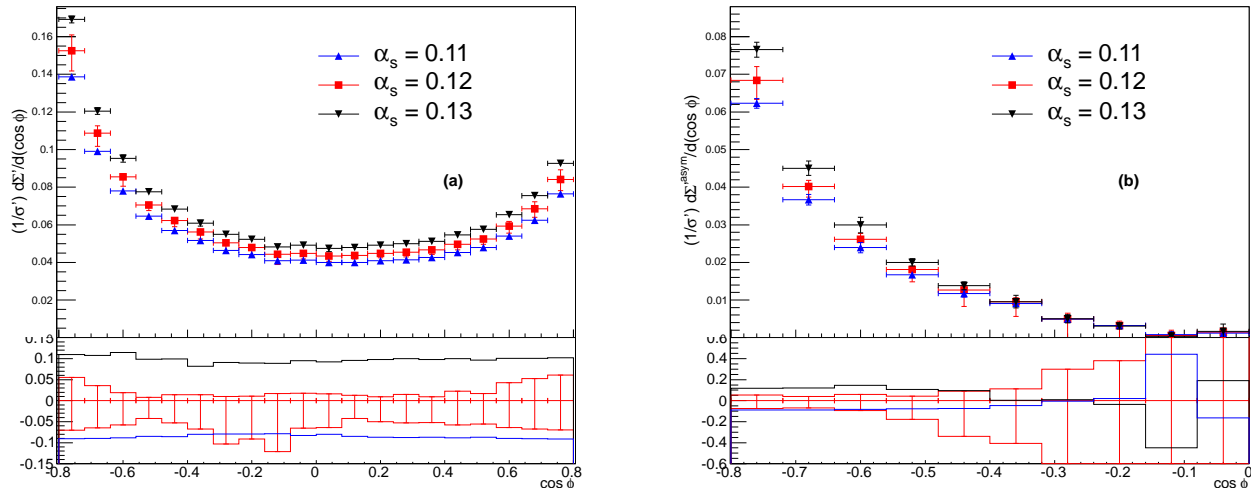


FIG. 8. (color online) Transverse EEC cross section (a) and its asymmetry (b) with three values of  $\alpha_s(M_Z) = 0.11$  (blue),  $= 0.12$  (red), and  $= 0.13$  (black). The bottom panel of the figures demonstrate the size of errors (red) and deviations with the values of  $\alpha_s(M_Z) = 0.11$  (blue) and  $= 0.13$  (black) from the results evaluated with  $\alpha_s = 0.12$ .

(in units of  $10^{-3}$ ), in which the last four bins contribute very little:

$$\frac{\alpha_s(m_Z)}{\langle \frac{1}{\sigma'} \frac{d\Sigma'^{asymm}}{d\phi} \rangle} \left| \begin{array}{c|c|c|c} 0.11 & 0.12 & 0.13 & \\ \hline 13.6^{+0.2}_{-1.4} & 14.8^{+0.3}_{-1.5} & 16.4^{+0.4}_{-1.6} & \end{array} \right.$$

Details of the calculations and numerical results for other values of the parameter  $R$ , cuts on  $p_{T\min}$ , and the center-of-mass energies for the LHC and the Tevatron will be published elsewhere.

#### IV. SUMMARY

To summarize, we have presented for the first time NLO results for the transverse EEC and its asymmetry for jets at the LHC. These distributions are shown to have all the properties that are required for the precision tests of perturbative QCD. In particular, they (i) are almost independent of the structure functions, with typical uncertainties at 1%, (ii) show weak scale sensitivity; varying the scale from  $\mu = E_T/2$  to  $\mu = 2E_T$ , the uncertainties are less than 5% with the current (NLO) theoretical accuracy, (iii) their dependence on modeling the underlying minimum bias events for judicious choice of the parameter  $R$  is likewise mild, ranging typically from 2% to 5% as one varies from  $R = 0.4$  to  $R = 0.6$ , and (iv) preserve sensitivity to  $\alpha_s(M_Z)$ ; varying  $\alpha_s(M_Z) = 0.11$  to  $0.13$ , the transverse EEC (AEEC) cross section changes approximately by 20% (15%), and thus these distributions will prove to be powerful techniques for the quantitative study of event shape variables and in the measurement of  $\alpha_s(M_Z)$  in hadron colliders.

#### ACKNOWLEDGEMENT

We thank Zoltan Nagy for providing us his NLOJET++ code and helpful discussions. We also thank Jan Kotanski for his help in the implementation of this program. Communications with Gavin Salam and Markus Wobisch are also

thankfully acknowledged. W. W. is supported by the Alexander-von-Humboldt Stiftung.

- 
- [1] K. Nakamura *et al.* [Particle Data Group], *J. Phys. G* **37**, 075021 (2010).
  - [2] For a review of recent QCD results from the Tevatron, see, for example, M. Wobisch, *Nucl. Phys. B Proc. Suppl.* (2012) (in press) and arXiv:1202.0205 [hep-ex].
  - [3] S. Chatrchyan *et al.* [CMS Collaboration], arXiv:1204.0696 [hep-ex].
  - [4] G. Aad *et al.* [Atlas Collaboration], *Eur. Phys. J. C* **71**, 1512 (2011) [arXiv:1009.5908 [hep-ex]].
  - [5] S. Catani, Y. L. Dokshitzer, M. H. Seymour and B. R. Webber, *Nucl. Phys. B* **406**, 187 (1993).
  - [6] S. Catani and M. H. Seymour, *Nucl. Phys. B* **485**, 291 (1997) [Erratum-ibid. B **510**, 503 (1998)]; [arXiv:hep-ph/9605323].
  - [7] M. Cacciari, G. P. Salam and G. Soyez, *JHEP* **0804**, 063 (2008) [arXiv:0802.1189 [hep-ph]].
  - [8] S. Catani and M. H. Seymour, *Phys. Lett. B* **378**, 287 (1996) [arXiv:hep-ph/9602277].
  - [9] Z. Nagy, *Phys. Rev. Lett.* **88**, 122003 (2002) [arXiv:hep-ph/0110315]; *Phys. Rev. D* **68**, 094002 (2003) [arXiv:hep-ph/0307268].
  - [10] A. Banfi, G. P. Salam and G. Zanderighi, *JHEP* **0408**, 062 (2004) [arXiv:hep-ph/0407287]; *JHEP* **1006**, 038 (2010) [arXiv:1001.4082 [hep-ph]].
  - [11] T. Aaltonen *et al.* [CDF Collaboration], *Phys. Rev. D* **83**, 112007 (2011) [arXiv:1103.5143 [hep-ex]].
  - [12] V. Khachatryan *et al.* [CMS Collaboration], *Phys. Lett. B* **699**, 48 (2011) [arXiv:1102.0068 [hep-ex]].
  - [13] G. Aad *et al.* [ATLAS Collaboration], arXiv:1206.2135 [hep-ex].
  - [14] T. Sjostrand, S. Mrenna and P. Z. Skands, *JHEP* **0605**, 026 (2006) [arXiv:hep-ph/0603175].
  - [15] T. Sjostrand, S. Mrenna and P. Z. Skands, *Comput. Phys. Commun.* **178**, 852 (2008) [arXiv:0710.3820 [hep-ph]].
  - [16] M. Bahr *et al.*, *Eur. Phys. J. C* **58**, 639 (2008) [arXiv:0803.0883 [hep-ph]]; arXiv:1102.1672 [hep-ph].
  - [17] A. Ali, E. Pietarinen and W. J. Stirling, *Phys. Lett. B* **141**, 447 (1984).
  - [18] C. L. Basham, L. S. Brown, S. D. Ellis and S. T. Love, *Phys. Rev. Lett.* **41**, 1585 (1978); *Phys. Rev. D* **19**, 2018 (1979).
  - [19] A. Ali and F. Barreiro, *Phys. Lett. B* **118**, 155 (1982); *Nucl. Phys. B* **236**, 269 (1984).
  - [20] D. G. Richards, W. J. Stirling and S. D. Ellis, *Nucl. Phys. B* **229**, 317 (1983).
  - [21] A. Ali and G. Kramer, *Eur. Phys. J.* **H36**, 245 (2011) [arXiv:1012.2288 [hep-ph]].
  - [22] See, for instance, Z. Bern *et al.*, arXiv:1112.3940 [hep-ph].
  - [23] A. D. Martin, W. J. Stirling, R. S. Thorne and G. Watt, *Eur. Phys. J. C* **63**, 189 (2009).
  - [24] H. L. Lai *et al.*, *Phys. Rev. D* **82**, 074024 (2010).
  - [25] P. Nason, *JHEP* **0411**, 040 (2004) [arXiv:hep-ph/0409146].
  - [26] S. Frixione, P. Nason and C. Oleari, *JHEP* **0711**, 070 (2007) [arXiv:0709.2092 [hep-ph]].
  - [27] We are aware of the ongoing NLL/NLO matching project within MATCHBOX: S. Platzer and S. Gieseke, arXiv:1109.6256 [hep-ph]. Private communications with Judith Katzy, Jan Kotanski and Simon Plaetzer are acknowledged.
  - [28] A. Banfi, G. P. Salam and G. Zanderighi, *JHEP* **0503**, 073 (2005) [arXiv:hep-ph/0407286].
  - [29] J. Beringer *et al.* [Particle Data Group Collaboration], *Phys. Rev. D* **86**, 010001 (2012).